 doi:10.20944/preprints202202.0010.v1

Article

Efficiency of positron-emission tomography with ^{18}F-DOPA for visualization of dophaminergency system of brain

Ksenia Tutsenko[2], Alina Khoroshavina[3], Vladislav Abramov[4], Mariia Tunik[4], Tatiana Anuchina[2], Natalia Malchik[2] Dmitry Pokhabov[2,4], Anastasiya Savelyeva[2,4] and Michael Sadovsky[1,2,4]*

[1] Institute of computational modelling SB RAS; msad@icm.krasn.ru
[2] V.F. Voino-Yasenetsky Krasnoyarsk state medical university
[3] Almazov Center
[4] Federal Research & Clinic Center of FMBA of Russia
* Correspondence: msad@icm.krasn.ru; Cell tel.: +7-902-990-4597 (M.S.)

Abstract: Positron-emission tomography is powerful but costly tool for various medical investigations. In particular, it is used in Parkinsons disease and essential tremor diagnostics. However, yet there is no standardized figures of the references, for it. We examined the PET efficiency for the analysis of development and degradation of dophaminergic neurons in Parkinsons disease. The informative indices are determined from the observed PET data. Also, high efficiency of PET for Parkinsons disease as approved.

Keywords: elastic map, clustering, classification, degeneration, diagnostics

1. Introduction

Parkinson's disease (PD) is among the most common neurodegenerative diseases of the elderly. PD is rare among youth [1]; however, the disease rate grows in a population elder than 60 [2,3]. Also, the decrease in the average age of the patients makes the problem worse. Men suffer from this pathology at a twice higher rate than women [4], although paper [5] reports an absence of the difference between genders in the disease rating.

The etiology of PD is still unknown in detail; late age, a family history of PD, exposure to adverse environmental factors are among risk factors [6,7]. The pathogenesis of PD is associated with neuron death, and these neurons are the most crucial component of the extrapyramidal system producing dopamine. At an early stage of the disease, the most significant loss of dopaminergic neurons is observed in the area of the ventrolateral substantia nigra; a progression of the disease causes the expansion of the neurodegenerative processes [8]. Also, PD is peculiar for accumulating an intracellular protein (α-synuclein). Lewy bodies, consisting of aggregated α-synuclein, are increased in number in cholinergic and monoaminergic neurons of the brain stem and neurons of the olfactory system [9,10]. The death of dopaminergic neurons at an early stage of the disease does not manifest in motor symptoms [11,12].

Positron emission tomography (PET) is an up-to-date and promising method in diagnosing PD and other diseases [13]. The registration of γ quanta emitted in the annihilation of an electron and a positron emitted by a radiopharmaceutical (RP) stands behind the method. RP consists of a biologically active substance (BAS) labelled with a positron-emitting radioisotope. One must adequately choose RP for successful PET diagnostics: it must be actively metabolized by a specific organ or a neoplasm [14,15]. The isotope used in RP must have a short half-life period, and tissues must weakly absorb its radiation. It is necessary to ensure a minimal radiation load on a human body and a high resolution of the recorded image. PET is advantageous in diagnosing PD in terms of high sensitivity to the metabolic changes in the target structures before the onset of atrophy. PET-examination in PD diagnosis unambiguously allows determining

Preprints (www.preprints.org) | NOT PEER-REVIEWED | Posted: 1 February 2022 doi:10.20944/preprints202202.0010.v1

the lack of dopamine, which is the key link in the pathogenesis of this disease. It detects the disease even at the early stages of its development [16].

2. Materials and Methods

^{18}F-DOPA is the optimal RP for studying the dopaminergic system. The substance is levodopa labelled with fluorine-18. Levodopa is an amino acid, an immediate precursor of dopamine able to cross the blood-brain barrier using a carrier. ^{18}F-DOPA binds to the decarboxylase of aromatic amino acids and generates positronic release [17].

The ratio of the ^{18}F-DOPA activity in the shell to the activity in the caudate nucleus is about 1 for healthy people. PD patients have this ratio close to 0.6 [18,19]. During the latency period and in the early stage of PD development, a decrease in the uptake of ^{18}F-DOPA is observed precisely in the dorsocaudal part of the shell on the contralateral side, i. e., in the side opposite to clinical manifestations. Similar changes are detected on the ipsilateral side, i. e.in the side of clinical symptoms occurrence, but to a lower extent, reflecting the neurodegenerative process's asymmetry [20].

Increasing the efficiency of differential diagnosis of PD and essential tremor (ET) is a hot topic of up-to-date neurology. The etiology and pathogenesis of ET are unknown in detail, and the most evident symptoms include tremors of the limbs, trunk, and vocal cords [21]. ET is also characterized by non-motor symptoms such as cognitive and affective disorders, sensory impairments, and dyssomnia [22,23]. Clinical practice follows several criteria for diagnosing ET and PD, but the incidence of erroneous diagnoses in some studies reaches 50 % [24,25]. This problem can be solved through examination of the dopaminergic system of the brain using PET with ^{18}F-DOPA. Detection of a decrease in the activity of this RP allows to suspect a patient to have PD; on the contrary, no destruction of dopaminergic neurons is observed for ET patients. Also, ^{18}F-DOPA can be used for the differential diagnostics of idiopathic parkinsonism and atypical parkinsonism. To do it, the zonal analysis of the striatum is used in a PET scan with ^{18}F-DOPA. Idiopathic Parkinson's syndrome mainly manifests in a more linear decrease in DA metabolism from the anterior to the posterior part of the shell [26].

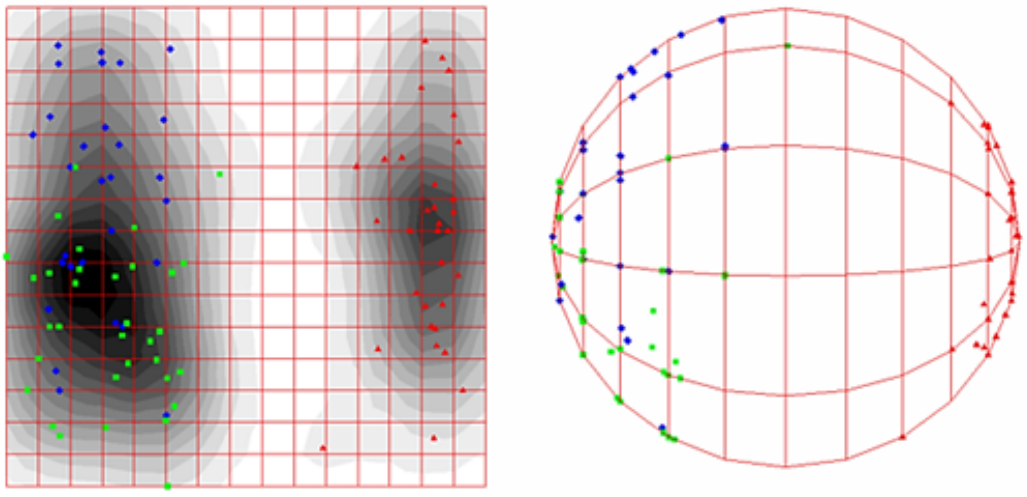

Figure 1. Elastic maps of the distribution of healthy people (green labels) vs. ET patients (blue labels) and PD patients (red labels) developed over 8 indicators of ^{18}F-DOPA activity.

The work was done from 2017 to 2020 in the Federal Siberian Research and Clinical Center of the FMBA of Russia in Krasnoyarsk. All patients initially underwent magnetic resonance imaging (MRI) of the brain to exclude structural changes and compare the MRI and PET images. Fifty minutes after the administration of ^{18}F-DOPA, static 3D scanning was performed for 20 minutes on a PET scanner. We analysed the maximum (*max*) and mean (*ave*) values of activity, measured in kilobecquerels per millilitre (kBq/ml), as well

 doi:10.20944/preprints202202.0010.v1

as the normalized indicators: the ratio of the activity of the shell / visual cortex (*SOR*), caudate/visual cortex (*COR*), posterior shell / front shell (*PAR*). Also, the ratio of the in-shell activity to the activity in the caudate nucleus (*SCR*) was recorded. All indicators were recorded from the right (**R**) and left (**L**) sides.

We use a Microsoft Excel database to store and process the collected data. The Shapiro-Wilk test was used for the normality of the distribution verification. Student's test was used to compare two groups if the distribution of values in both groups were normal. If the distribution within at least one group under study differed from the normal one, the Mann-Whitney test was used for comparison. The significance level for all of the above criteria was set to $\alpha = 0.05$. ROC analysis was used to assess the quality of the binary classification. Data were analysed using the IBM SPSS Statistics 26 software. The elastic maps method [27] was used to visualize multidimensional data. We use freely distributed VidaExpert software[1]. The diagnostic norm was determined using smoothed curves constructed with the Parsen – Rosenblatt window method in the Rstudio software.

3. Results

We have selected the most informative indicators to distinguish the groups of patients. To do it, we use the Mann-Whitney and the Student's tests and ROC analysis. We measured the absolute values of the average activity of ^{18}F-DOPA in the posterior shell (PPRave, PPLave) and the visual cortex on both sides (ORave, OLave). The SOR, COR, SCR, and PAR indices are calculated as the ratio of the average values of the activities in different zones. These indices were selected from the entire set of relative indices due to their increased informativity.

The level of RP uptake in the rear part of the shell is the most diagnostically significant indicator among all relative indices. The shell plays an essential role in regulating motor activity through interaction with the caudate nucleus, globus pallidus, and substantia nigra. Dysfunction of the nigrostriatal dopaminergic pathway is specific for PD. In particular, there is a sharp decrease in the DA release level from the striatal terminals [28]. The brain shell contains the largest number of dopaminergic neurons; papers[25,29] report the start of the pathological process from this section.

From the moment of synthesis to the moment of the injection of RP to a patient, some time passes, varying within a certain period. ^{18}F has a relatively short half-life ($T_{\frac{1}{2}} = 110$ minutes), so each person receives a different number of radioactive fluorine atoms. It follows in the variability of the data. It may affect the diagnostic accuracy of absolute and relative indicators measurement.

SOR is the most diagnostically valuable indicator. It is associated with the most significant difference in RP accumulation in the shell and the visual cortex. The visual cortex has no dopaminergic neurons, or they are present in insignificant amounts; therefore, the indicator of RP activity in this section is very low. The diagnostic value of SCR and COR is slightly lower because of the minor difference between the accumulation in the shell and the caudate nucleus (SCR), the caudate nucleus, and the visual cortex (COR). It makes the relative indicators of great diagnostic value since they eliminate the disadvantages of the absolute figures, which may not be accurate due to the treatment protocol's details.

The elastic maps method was used to visualize multidimensional data. Two separate clusters appear in constructing elastic maps using eight selected relative indicators with the highest diagnostic value (figure 1). The spherical map also approves the absence of merging the clusters into one. Healthy people and ET patients form separate clusters. It may result from the fact that dopaminergic neurons death is not observed in ET; this cluster opposes the cluster of PD patients.

[1] http://bioinfo-out.curie.fr/projects/vidaexpert/

Preprints (www.preprints.org) | NOT PEER-REVIEWED | Posted: 1 February 2022 doi:10.20944/preprints202202.0010.v1

Eight relative indicators, SOR (PPRave / ORave), SOR (PPLave / OLave), COR (NCRave / ORave), COR (NCLave / OLave), SCR (PPRave / NCRave), SCR (PPLave / NCLave), PAR (PPRave / APLave), PAR (PPLave / APLave), have the highest value for PD diagnosing.

Table 1. Indicators of diagnostic significance based on ROC analysis for certain thresholds; confidence interval is 95 %, q is threshold value.

Index	Se %	Sp %	Acc %	q
SOR (APRave/ORave)	81.25 (64.69 %; 91.11 %)	81.82 (65.61 %; 91.39 %)	81.54 (75.02 %; 84.54 %)	2.56
SOR (APLmax/Olmax)	78.13 (61.25 %; 88.98 %)	81.82 (65.61 %; 91.39 %)	80.00 (73.43 %; 83.22 %)	2.40
SOR (APLave/Olave)	81.25 (64.69 %; 91.11 %)	81.82 (65.61 %; 91.39 %)	81.54 (75.02 %; 84.54 %)	2.55
SOR (PPRmax/ORmax)	84.38 (68.25 %; 93.14 %)	84.85 (69.08 %; 93.35 %)	84.62 (78.22 %; 87.14 %)	2.16
SOR (PPRave/ORave)	84.38 (68.25 %; 93.14 %)	84.85 (69.08 %; 93.35 %)	84.62 (78.22 %; 87.14 %)	2.23
SOR (PPLmax/OLmax)	84.38 (68.25 %; 93.14 %)	84.85 (69.08 %; 93.35 %)	84.62 (78.22 %; 87.14 %)	2.15
SOR (PPLave/OLave)	84.38 (68.25 %; 93.14 %)	84.85 (69.08 %; 93.35 %)	84.62 (78.22 %; 87.14 %)	2.24
SCR (APRmax/NCRmax)	81.25 (64.69 %; 91.11 %)	78.79 (62.25 %; 89.32 %)	80.00 (73.43 %; 83.22 %)	1.021
SCR (APLmax/NCLmax)	78.13 (61.25 %; 88.98 %)	81.82 (65.61 %; 91.39 %)	80.00 (73.43 %; 83.22 %)	1.076
SCR (APLave/NCLave)	81.25 (64.69 %; 91.11 %)	81.82 (65.61 %; 91.39 %)	81.54 (75.02 %; 84.54 %)	1.074
SCR (PPRmax/NCRmax)	84.38 (68.25 %; 93.14 %)	81.82 (65.61 %; 91.39 %)	83.08 (76.61 %; 85.85 %)	0.909
SCR (PPRave/NCRave)	84.38 (68.25 %; 93.14 %)	84.85 (69.08 %; 93.35 %)	84.62 (78.22 %; 87.14 %)	1.024
SCR (PPLmax/NCLmax)	84.38 (68.25 %; 93.14 %)	84.85 (69.08 %; 93.35 %)	84.62 (78.22 %; 87.14 %)	0.973
SCR (PPLave/NCLave)	84.38 (68.25 %; 93.14 %)	84.85 (69.08 %; 93.35 %)	84.62 (78.22 %; 87.14 %)	0.920
PAR (PPLmax/APLmax)	84.38 (68.25 %; 93.14 %)	81.82 (65.61 %; 91.39 %)	83.08 (76.61 %; 85.85 %)	0.915

The high cost of investigation and the labor-consuming investigation procedure resulted in a considerably small number of patients and healthy people involved in the study. It follows in smoothing the raw data due to the Parzen–Rozenblatt technique. It is the method of the non-parametric reconstruction of the distribution density with a finite sample [30,31].

We have used two methods to define the diagnostic norm: the former is mainly visual. It uses a plot of the distribution density of RP activity in healthy people vs. PD patients (see Fig. 2). The latter is based on ROC analysis. We used the Parsen-Rosenblatt smoothing for the first method implementation. The abscissa x shows the activity of ^{18}F-DOPA $\times$ measured in kBq/ml; the distribution density $f(x)$ is plotted on the ordinate. The intersection point of the curves where the probability of a patient to be healthy is equal to the probability that the patient is sick is stipulated the left border of the norm. The indicators exhibiting the curves of activity of ^{18}F-DOPA for the group of healthy people and the group of PD patients with PD with large intersection areas were excluded from the analysis (see Fig. 3). Thus, we have determined six relative figures with the low intersecting charts of the density distribution, with apparent identification of the norm of RP activity, see Table 2

Preprints (www.preprints.org) | NOT PEER-REVIEWED | Posted: 1 February 2022 doi:10.20944/preprints202202.0010.v1

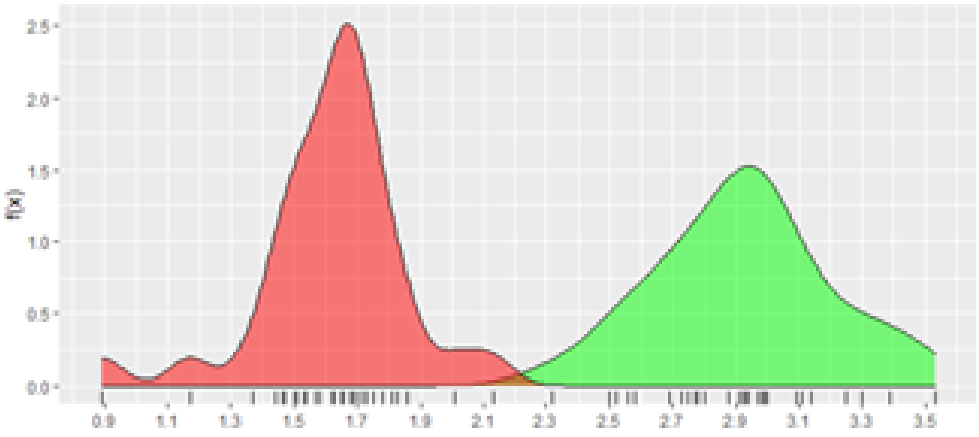

(a)

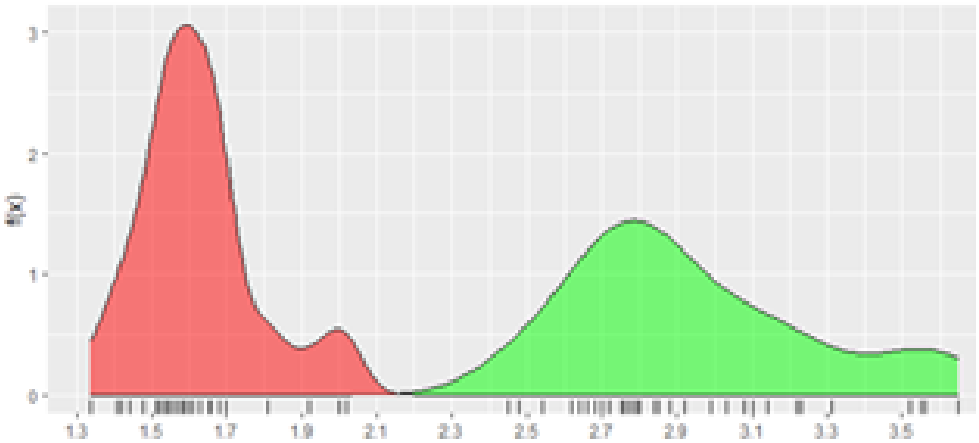

(b)

Figure 2. The curves for SOR (PPRave/ORave) (A) and SOR (PPLave/OLave) (B) (healthy people are shown in green, and PD patients are shown in red).

Table 2. The proposed norm values for the indices with good differentiation of healthy people vs. PD patients.

Index	The proposed norm, kBq/ml
SOR (PPRave/ORave)	$\geq$ 2.20
SOR (PPLave/OLave)	$\geq$ 2.15
SCR (PPRave/NCRave)	$\geq$ 1.01
SCR (PPLave/NCLave)	$\geq$ 0.95
PAR (PPRave/APRave)	$\geq$ 0.90
PAR (PPLave/APLave)	$\geq$ 0.92

Another way to determine diagnostic norms is the ROC analysis. This method is implied if two outputs are expected: the former comprises the positive outputs (a patient is sick), and the latter comprises the negative outputs (a patient is healthy). ROC-curve shows the dependence of the number truly classified positive outputs (true positive set) on the number of the false-negative outputs (false positive outputs set) [32,33]. A variation of the threshold yields a separation into two classes, thus providing a researcher with selectivity (Se), specificity (Sp), and accuracy (Acc), see Table 1. The maximal values of sensitivity (Se) and specificity (Sp) of the binary classification are stipulated to be a threshold, thus referred to as the norm. Table 1 shows the norms of indicators distinguishing healthy people from the patients with Parkinson's disease with an accuracy (Acc) above 80 %.

Preprints (www.preprints.org) | NOT PEER-REVIEWED | Posted: 1 February 2022 doi:10.20944/preprints202202.0010.v1

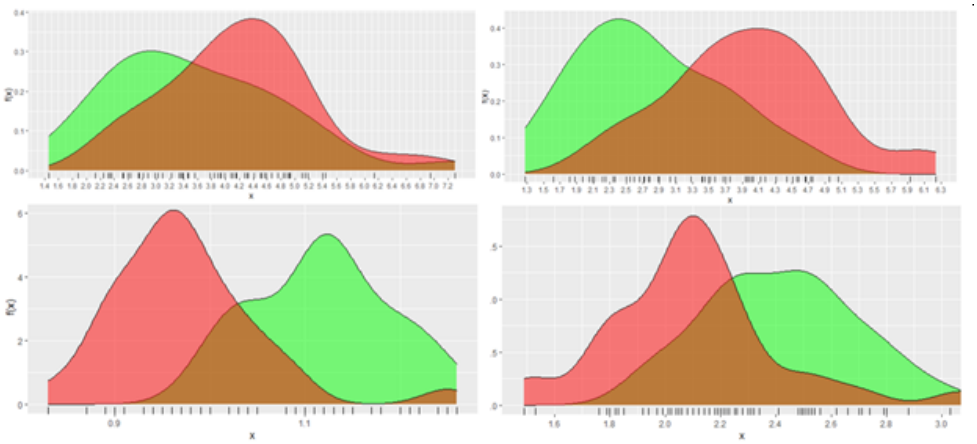

Figure 3. Examples of the curves representing the excluded indices (healthy people are shown in green, and PD patients are shown in red).

Some subjectivity may in the visual determination of the threshold value cause a bias in the determination of the diagnostic norm when the first method is used. The technique implies a smoothing of the curves that also may reduce the accuracy. ROC analysis is free from the above disadvantages since threshold values are determined based on the numerical values of indicators of diagnostic significance (Se, Sp, Acc). The graphical method to determine the threshold values yields the visual assessment of the power of some indicators to differentiate the groups, while the ROC analysis supports this evaluation numerically.

RP activity indicators observed in different brain areas successfully differentiate PD patients from healthy people and ET patients. Statistically significant differences between healthy and PD patients were found in RP activity of the posterior shell, visual cortex, for all relative parameters. ET patients and PD patients groups exhibit significant differences in the anterior and posterior shells of the visual cortex for all relative indicators. The ROC analysis makes it diagnostically valuable to study the activity of ^{18}F-DOPA in the posterior shell and visual cortex; relative indicators are of the most significant diagnostic value.

Elastic maps identify two separate clusters. Healthy people and patients with ET form the first cluster, and the second cluster consists of patients with PD. Thus, out of 40 analysed indicators, 8 most diagnostically significant were selected, these include: SOR (PPRave / ORave), SOR (PPLave / OLave), COR (NCRave / ORave), COR (NCLave / OLave), SCR (PPRave / NCRave), SCR (PPLave / NCLave), PAR (PPRave / APLave), PAR (PPLave / APLave). The graphs of the distribution density of the RP activity in healthy people and patients with PD were plotted. For the indicators, the graphs with the minimum intersection zones, diagnostic norms were determined.

4. Conclusions

Here we present the reference values of the indices for brain PET investigation, at least for Russia; the reference may differ for various countries. The choice and verification of these indices values are approved with two independent methods: the former is the method of Parzen–Rosenblat smoothening curve implementation, and the latter is ROC analysis. These methods have been used for their advantages: they provide efficient visualisation and support an objective evaluation of the obtained reference values of indices. The methods could be highly applied due to the efficiency in the differential diagnosis of PD vs. ET. That latter disease is not related to dopaminergic shortage. Standard diagnostics techniques fail to differ these nosologies making the proposed methods valuable for the up-to-date routine practice in clinics. Additionally, implementing the indices in relative scale makes the indices universal and indepen-

dent on the peculiarities of the medical investigation protocol and hardware used for investigation.

Author Contributions: Conceptualization, V.A. and D.P.; methodology, V.A., K.T., A.Kh. and M.S.; statistical analysis and data retrieval, K.T., A.Kh., T.A. N.M. and M.T.; software, computations and visualization, K.T., A.Kh. and M.T.; writing, M.S, V.A. and D.P. All authors have read and agreed to the published version of the manuscript.

Funding: This research received no external funding.

Conflicts of Interest: The authors declare no conflict of interest.

References

1. Twelves, D.; Perkins, K.S.; Counsell, C. Systematic review of incidence studies of Parkinson's disease. *Movement disorders: official journal of the Movement Disorder Society* **2003**, *18*, 19–31.
2. Van Den Eeden, S.K.; Tanner, C.M.; Bernstein, A.L.; Fross, R.D.; Leimpeter, A.; Bloch, D.A.; Nelson, L.M. Incidence of Parkinson's disease: variation by age, gender, and race/ethnicity. *American journal of epidemiology* **2003**, *157*, 1015–1022.
3. Schrag, A.; Münchau, A.; Bhatia, K.; Quinn, N.; Marsden, C. Essential tremor: an overdiagnosed condition? *Journal of neurology* **2000**, *247*, 955–959.
4. Baldereschi, M.; Di Carlo, A.; Rocca, W.A.; Vanni, P.; Maggi, S.; Perissinotto, E.; Grigoletto, F.; Amaducci, L.; Inzitari, D.; others. Parkinson's disease and parkinsonism in a longitudinal study: two-fold higher incidence in men. *Neurology* **2000**, *55*, 1358–1363.
5. Kusumi, M.; Nakashima, K.; Harada, H.; Nakayama, H.; Takahashi, K. Epidemiology of Parkinson's disease in Yonago City, Japan: comparison with a study carried out 12 years ago. *Neuroepidemiology* **1996**, *15*, 201–207.
6. Ascherio, A.; Schwarzschild, M.A. The epidemiology of Parkinson's disease: risk factors and prevention. *The Lancet Neurology* **2016**, *15*, 1257–1272.
7. Noyce, A.J.; Bestwick, J.P.; Silveira-Moriyama, L.; Hawkes, C.H.; Giovannoni, G.; Lees, A.J.; Schrag, A. Meta-analysis of early nonmotor features and risk factors for Parkinson disease. *Annals of neurology* **2012**, *72*, 893–901.
8. Damier, P.; Hirsch, E.; Agid, Y.; Graybiel, A. The substantia nigra of the human brain: II. Patterns of loss of dopamine-containing neurons in Parkinson's disease. *Brain* **1999**, *122*, 1437–1448.
9. Berman, S.B.; Miller-Patterson, C. PD and DLB: Brain imaging in Parkinson's disease and dementia with Lewy bodies. *Progress in molecular biology and translational science* **2019**, *165*, 167–185.
10. Braak, H.; Del Tredici, K.; Rüb, U.; De Vos, R.A.; Steur, E.N.J.; Braak, E. Staging of brain pathology related to sporadic Parkinson's disease. *Neurobiology of aging* **2003**, *24*, 197–211.
11. Dijkstra, A.A.; Voorn, P.; Berendse, H.W.; Groenewegen, H.J.; Bank, N.B.; Rozemuller, A.J.; van de Berg, W.D. Stage-dependent nigral neuronal loss in incidental Lewy body and Parkinson's disease. *Movement disorders* **2014**, *29*, 1244–1251.
12. Iacono, D.; Geraci-Erck, M.; Rabin, M.L.; Adler, C.H.; Serrano, G.; Beach, T.G.; Kurlan, R. Parkinson disease and incidental Lewy body disease: just a question of time? *Neurology* **2015**, *85*, 1670–1679.
13. Löhle, M.; Wolz, M.; Beuthien-Baumann, B.; Oehme, L.; van den Hoff, J.; Kotzerke, J.; Reichmann, H.; Storch, A. Olfactory dysfunction correlates with putaminal dopamine turnover in early de novo Parkinson's disease. *Journal of Neural Transmission* **2020**, *127*, 9–16.
14. Hilker, R.; Schweitzer, K.; Coburger, S.; Ghaemi, M.; Weisenbach, S.; Jacobs, A.H.; Rudolf, J.; Herholz, K.; Heiss, W.D. Nonlinear progression of Parkinson disease as determined by serial positron emission tomographic imaging of striatal fluorodopa F 18 activity. *Archives of neurology* **2005**, *62*, 378–382.
15. Savica, R.; Grossardt, B.R.; Bower, J.H.; Ahlskog, J.E.; Rocca, W.A. Incidence and pathology of synucleinopathies and tauopathies related to parkinsonism. *JAMA neurology* **2013**, *70*, 859–866.
16. Dyukarev, V. Positron emission tomography: the essence of the method, advantages and disadvantages. *Bjulleten' medicinskih internet konferencij* **2013**, *11*, 1196.
17. Jokinen, P.; Helenius, H.; Rauhala, E.; Brück, A.; Eskola, O.; Rinne, J.O. Simple ratio analysis of ^{18}F-fluorodopa uptake in striatal subregions separates patients with early Parkinson disease from healthy controls. *Journal of Nuclear Medicine* **2009**, *50*, 893–899.

18. Granov, A.; Tyutin, L.; Stanzhevskii, A. The application of nuclear medicine imaging in neurology, neurosurgery and psychiatry. *Annals of the Russian academy of medical sciences* **2012**, *67*, 13–18.
19. Stanzhevsky, A.; Tyutin, L.; Litvinenko, I. The application of positron emission tomography in Parkinson's disease diagnosis. *Radiation diagnostics and therapy* **2010**, pp. 12–19.
20. Katunina, E.; Ilina, E.; Sadekhova, G.; Gaisenuk, E. Approaches to early diagnosis of Parkinson's disease. *S.S. Korsakov Journal of Neurology and Psychiatry* **2019**, *119*, 119–127.
21. Critchley, E. Clinical manifestations of essential tremor. *Journal of Neurology, Neurosurgery & Psychiatry* **1972**, *35*, 365–372.
22. Klaming, R.; Annese, J. Functional anatomy of essential tremor: lessons from neuroimaging. *American Journal of Neuroradiology* **2014**, *35*, 1450–1457.
23. Louis, E.D.; Diaz, D.T.; Kuo, S.H.; Gan, S.R.; Cortes, E.P.; Vonsattel, J.P.G.; Faust, P.L. Inferior Olivary nucleus degeneration does not lessen tremor in essential tremor. *Cerebellum & ataxias* **2018**, *5*, 1–10.
24. Jain, S.; Lo, S.E.; Louis, E.D. Common misdiagnosis of a common neurological disorder: how are we misdiagnosing essential tremor? *Archives of neurology* **2006**, *63*, 1100–1104.
25. Selikhova, M.; Selikhova, M.; Katunina, E.; Katunina, E.; Whone, A.; Whone, A. PET and SPECT in the assessment of monoaminergic brain systems in extrapyramidal disorders. *Annals of clinical and experimental neurology* **2019**, *13*.
26. Stormezand, G.N.; Chaves, L.T.; García, D.V.; Doorduin, J.; De Jong, B.M.; Leenders, K.L.; Kremer, B.P.; Dierckx, R.A. Intrastriatal gradient analyses of ^{18}F-FDOPA PET scans for differentiation of Parkinsonian disorders. *NeuroImage: Clinical* **2020**, *25*, 102161.
27. Zinovev, A.; Pitenko, A. Visualization of data using elastic maps. *Radio Electronics, Computer Science, Control* **2000**.
28. Fukunaga, K. *Introduction to statistical pattern recognition*; Elsevier, 2013.
29. Oehme, L.; Perick, M.; Beuthien-Baumann, B.; Wolz, M.; Storch, A.; Löhle, M.; Herting, B.; Langner, J.; van den Hoff, J.; Reichmann, H.; others. Comparison of dopamine turnover, dopamine influx constant and activity ratio of striatum and occipital brain with 18 F-dopa brain PET in normal controls and patients with Parkinson's disease. *European journal of nuclear medicine and molecular imaging* **2011**, *38*, 1550–1559.
30. Parzen, E. On estimation of a probability density function and mode. *The annals of mathematical statistics* **1962**, *33*, 1065–1076.
31. Davis, R.A.; Lii, K.S.; Politis, D.N. Remarks on some nonparametric estimates of a density function. In *Selected Works of Murray Rosenblatt*; Springer, 2011; pp. 95–100.
32. Fawcett, T. An introduction to ROC analysis. *Pattern recognition letters* **2006**, *27*, 861–874.
33. Obuchowski, N.A. ROC analysis. *American Journal of Roentgenology* **2005**, *184*, 364–372.